Analysis of Faulted Power System with Fault Current Limiter Using Compensation Current Method

Rohit S. Thute*, Himanshu J. Bahirat†, Shrikrishna A. Khaparde‡
Department of Electrical Engineering, Indian Institute of Technology Bombay, Powai, Mumbai-400076, India
(email: rohitthute@ee.iitb.ac.in*, hjbahirat@ee.iitb.ac.in†,sak@ee.iitb.ac.in‡)

***Abstract*—Fault current limiters (FCL) keep the fault current levels below equipment ratings in expanding power systems. Analyzing a faulted power system with FCL using symmetrical components becomes computationally intensive due to the coupling between FCL impedance and the need to recalculate the bus impedance matrix. This paper proposes a fault analysis method based on compensation currents to minimize the computation efforts. The paper presents the mathematical formulation for the compensation currents to model a fault and an FCL. This paper discusses the coupling between sequence networks for various FCL activation cases and identifies corresponding interconnections. The results of the proposed method for various fault types and FCL activation are validated with time-domain simulations. In addition, the computational efforts required by the proposed method are discussed with an application to a large power system. The results show that the proposed method requires minimum computations. The analysis of FCLs with non-linear impedances is beyond the scope of this paper.**

***Index Terms*—Fault analysis, Fault current limiter, Sequence networks, Symmetrical components.**

I. Introduction

An increase in energy demand requires expansion of the existing grid with new energy resources. Such grid expansion increases the fault current levels of the grid. The increased fault levels beyond the rating of the existing equipment, such as circuit breakers, may lead to their failure [1]. In such situations, the existing equipment requires an upgrade to ensure reliable operation, which has economic implications. A cost-effective solution to this problem is a fault current limiter (FCL), which restricts the fault levels below the equipment rating. The FCL is a variable series impedance device that provides negligible impedance in normal operations and high impedance during fault [2]. Literature provides various studies on FCL application to the power system, such as to limit the fault current levels [3], improve transient recovery voltage [4], help generator circuit breakers avoid the occurrence of delayed current zeros [5], improve fault ride-through capability [6], and improve transient stability [7]. For such applications, the FCLs are being deployed in transmission systems [8] and distribution systems [9].

Submitted to the 23rd Power Systems Computation Conference (PSCC 2024).

Installation of such devices in the power system requires analysis tools to facilitate effective FCL parameter selection according to required fault current limits. In addition, such tools are also essential to identify the impacts of FCL on already installed protection systems [2] and help modify relay settings to eliminate ill impacts. One approach to study this is the time-domain approach with detailed FCL models. This approach becomes complex for large power systems and may be unnecessary for studies like protection feasibility and circuit breaker sizing. For such studies, an approach of fault analysis based on phasor calculations is more suitable. This approach is well known for analyzing conventional power systems [10] and is also extended to power systems with series compensated transmission lines [11], inverter-based resources [12], or FCLs [13], [14].

The classical fault analysis method based on symmetrical components faces the challenge of handling sequence network coupling introduced due to FCL impedance [13]. Previous papers [13] and [14], dealt with fault analysis of power systems with various types of FCLs. In [13], the authors propose a fault analysis method for power systems with FCL, which requires recalculation of the bus impedance matrix for the positive sequence network considering FCL impedance. In [14], the authors propose a method to evaluate fault current for three-line and single-line to ground faults at FCL buses based on modified bus impedance matrix elements. In [15], authors formulated the problem of FCL parameter sizing to obtain the required fault current reduction.

The fault analysis methods proposed in [13] and [14], require recalculating the bus impedance matrix elements for each FCL impedance change. The recalculation of the bus impedance matrix is a computationally intensive process for large power systems, which can be avoided. The problem statement of this paper is to propose an analysis method for faulted power systems with FCL, which does not require recalculation of bus impedance matrix elements for each FCL impedance change. For this purpose, the paper proposes a compensation current based method to avoid recalculating the bus impedance matrix. The compensation method finds its application for analyzing modified networks [16] and in EMTP [17]. Following are the main contributions of this paper:

- Defined the sequence network interconnections introduced due to FCL impedance depending on its activation.

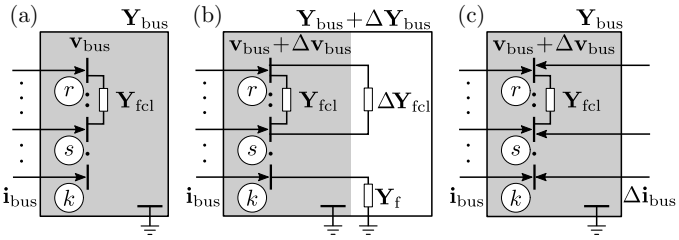

Fig. 1. System representation for mathematical formulation: (a) System with FCL in low impedance state, (b) Faulted system with FCL in high impedance state modeled with external branches $\Delta\mathbf{Y}_{\text{fcl}}$ and $\mathbf{Y}_{\text{f}}$, and (c) Faulted system with FCL in high impedance state modeled with proposed compensation current method.

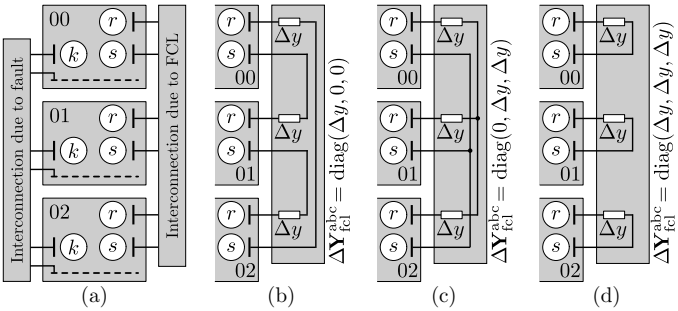

Fig. 2. (a) Sequence network interconnections considering simultaneously a fault and FCL impedance change; and sequence network interconnection due to (b) single-phase activation of FCL, (c) two-phase activation of FCL, and (d) all-phase activation of FCL.

- Proposed a method based on compensation currents to analyze faulted power systems with FCL.

The rest of the paper is structured as follows: Section II presents the mathematical formulation of the proposed method. Section III validates the proposed method with time-domain simulation results. Section IV discusses the computational effort of the proposed method and presents its application to the IEEE 118 bus system. Section V concludes the paper.

II. Proposed Method

This section first presents the coupling introduced during various FCL activation cases and identifies the corresponding sequence network interconnections. Later, the mathematical formulation of the proposed method is presented.

A. Coupling of Fault Current Limiter Impedance and Identification of Sequence Network Interconnections

Consider an n-bus power system with buses $\{r, s, k\}$ as shown in Fig. 1a. The FCL is connected between buses r and s. In pre-fault condition, the FCL is in a low impedance state with phase impedance z^{li} and is represented by a branch with balanced admittance of $\mathbf{Y}^{\text{abc}}_{\text{fcl}} = \text{diag}(\frac{1}{z^{\text{li}}}, \frac{1}{z^{\text{li}}}, \frac{1}{z^{\text{li}}})$. For a symmetrical network, this pre-fault network has no coupling between sequence networks. Now, consider a fault at bus k leading to FCL activation and change in its impedance. The FCL impedance transitions to high impedance value z^{hi} from z^{li} in phases with current higher than critical current rating. Fig. 1b represents this faulted power system, where the branch $\mathbf{Y}_{\text{f}}$ at bus k represents the fault admittance and the branch $\Delta\mathbf{Y}_{\text{fcl}}$ across buses r and s represents the change in FCL admittance. Here, the change in the FCL impedance is modeled by adding branch $\Delta\mathbf{Y}^{\text{abc}}_{\text{fcl}}$ across FCL buses r and s, such that the modified FCL impedance during fault is given by $(\mathbf{Y}^{\text{abc}}_{\text{fcl}}+\Delta\mathbf{Y}^{\text{abc}}_{\text{fcl}})^{-1}$.

The pre-fault network is symmetrical and hence can be represented by three decoupled sequence networks. During fault, the coupling of $\mathbf{Y}_{\text{f}}$ and $\Delta\mathbf{Y}_{\text{fcl}}$ introduce interconnections between these decoupled sequence networks as shown in Fig. 2a, where 00, 01 and 02 represent zero, positive and negative sequence, respectively. The fault branch $\mathbf{Y}_{\text{f}}$ introduces interconnections between bus k and reference bus; and the FCL branch $\Delta\mathbf{Y}_{\text{fcl}}$ introduces interconnections between buses r and s. The interconnections for various fault types are well known [10] and hence not discussed here. Following discussion presents the coupling of $\Delta\mathbf{Y}_{\text{fcl}}$ for various FCL activation cases and identifies corresponding sequence network interconnection.

TABLE I
$\Delta\mathbf{Y}^{012}_{\text{FCL}}$ FOR VARIOUS FCL ACTIVATION CASES.

Single-phase	Two-phase	All-phase
$\frac{\Delta y}{3}\begin{bmatrix}1&1&1\\1&1&1\\1&1&1\end{bmatrix}$	$\frac{\Delta y}{3}\begin{bmatrix}2&-1&-1\\-1&2&-1\\-1&-1&2\end{bmatrix}$	$\Delta y\begin{bmatrix}1&0&0\\0&1&0\\0&0&1\end{bmatrix}$

1) Single-phase activation: For FCL activation in phase A, the FCL impedance appears as $\mathbf{Z}^{\text{abc}}_{\text{fcl}} = \text{diag}(z^{\text{hi}}, z^{\text{li}}, z^{\text{li}})$. This impedance is modeled with branch of admittance $\Delta\mathbf{Y}^{\text{abc}}_{\text{fcl}} = \text{diag}(\Delta y, 0, 0)$, where $\Delta y = \frac{1}{z^{\text{hi}}} - \frac{1}{z^{\text{li}}}$. This admittance is converted to sequence domain as $\Delta\mathbf{Y}^{012}_{\text{fcl}}$ and is given in Table I. Matrix $\Delta\mathbf{Y}^{012}_{\text{fcl}}$ have off-diagonal elements which represent the coupling in sequence domain. Furthermore, the sequence network interconnection is identified based on relation between the sequence currents through the branch $\Delta\mathbf{Y}^{012}_{\text{fcl}}$. The sequence current $\Delta\mathbf{i}^{012}_r = [\Delta I^{00}_r, \Delta I^{01}_r, \Delta I^{02}_r]^{\text{T}}$ through $\Delta\mathbf{Y}^{012}_{\text{fcl}}$ is given as $\Delta\mathbf{i}^{012}_r = \Delta\mathbf{Y}^{012}_{\text{fcl}}(\mathbf{v}^{012}_r - \mathbf{v}^{012}_s)$, where $\mathbf{v}^{012}_r$ and $\mathbf{v}^{012}_s$ are sequence domain voltage across buses r and s, respectively. For $\Delta\mathbf{Y}^{012}_{\text{fcl}}$ with single-phase activation, $\Delta\mathbf{i}^{012}_r = \Delta\mathbf{Y}^{012}_{\text{fcl}}(\mathbf{v}^{012}_r - \mathbf{v}^{012}_s)$ leads to $\Delta I^{00}_r = \Delta I^{01}_r = \Delta I^{02}_r$ which indicates a series connection of sequence networks as shown in Fig. 2b.

2) Two-phase activation: For FCL activation in phases B and C, the FCL impedance appears as $\mathbf{Z}^{\text{abc}}_{\text{fcl}} = \text{diag}(z^{\text{li}}, z^{\text{hi}}, z^{\text{hi}})$. This impedance is modeled with branch of admittance $\Delta\mathbf{Y}^{\text{abc}}_{\text{fcl}} = \text{diag}(0, \Delta y, \Delta y)$. This admittance in sequence domain given in Table I for two-phase activation, which shows off-diagonal elements representing coupling. For $\Delta\mathbf{Y}^{012}_{\text{fcl}}$ with two-phase activation, $\Delta\mathbf{i}^{012}_r = \Delta\mathbf{Y}^{012}_{\text{fcl}}(\mathbf{v}^{012}_r - \mathbf{v}^{012}_s)$ leads to $\Delta I^{00}_r + \Delta I^{01}_r + \Delta I^{02}_r = 0$ which indicates a parallel connection of sequence networks as shown in Fig. 2c.

3) All-phase activation: For FCL activation in all phases, the FCL impedance appears as $\mathbf{Z}^{\text{abc}}_{\text{fcl}} = \text{diag}(z^{\text{hi}}, z^{\text{hi}}, z^{\text{hi}})$. This impedance is modeled with external branch of admittance $\Delta\mathbf{Y}^{\text{abc}}_{\text{fcl}} = \text{diag}(\Delta y, \Delta y, \Delta y)$. Matrix $\Delta\mathbf{Y}^{012}_{\text{fcl}}$ for all-phase

activation is given in Table I, which is diagonal matrix suggesting no coupling. Fig. 2d shows the sequence network interconnection for all-phase activation, where sequence networks are isolated after inclusion of $\Delta\mathbf{Y}_{\text{fcl}}^{012}$.

Above discussion demonstrated the coupling introduced during single-phase and two-phase FCL activation. Analyzing such systems with symmetrical components requires solving all three sequence networks simultaneously, which is computationally intensive. To reduce such computational effort, this paper proposes a fault analysis method based on compensation currents which is presented below.

B. Fault Analysis of System with Fault Current Limiter

The system in pre-fault condition shown in Fig. 1a can be represented by (1), where $\mathbf{i}_{\text{bus}}, \mathbf{v}_{\text{bus}} \in \mathbb{C}^{3n}$ and $\mathbf{Y}_{\text{bus}} \in \mathbb{C}^{3n\times 3n}$ represent bus current injection vector, bus voltage vector and bus admittance matrix in sequence domain, respectively. For further discussions, the superscript 012 is dropped for matrices and vectors in sequence domain. For a balanced pre-fault condition, $\mathbf{i}_{\text{bus}}$ only has positive sequence entries representing generator injections and $\mathbf{Y}_{\text{bus}}$ has no coupling between sequence networks. The system in fault condition shown in Fig. 1b is obtained by adding two external branches $\mathbf{Y}_{\text{f}}$ and $\Delta\mathbf{Y}_{\text{fcl}}$, as discussed earlier. Addition of these two external branches to the system changes the original bus admittance matrix to $(\mathbf{Y}_{\text{bus}}+\Delta\mathbf{Y}_{\text{bus}})$. The faulted power system in Fig. 1b can be represented by (2) assuming the generator current injections remain the same, which gives the modified bus voltages $(\mathbf{v}_{\text{bus}} + \Delta\mathbf{v}_{\text{bus}})$ during the fault with FCL activation. Solving (2) requires evaluating $(\mathbf{Y}_{\text{bus}}+\Delta\mathbf{Y}_{\text{bus}})^{-1}$ or solving system of $3n$ linear equations, which need to be avoided.

$$\mathbf{v}_{\text{bus}} = \mathbf{Y}_{\text{bus}}^{-1}\mathbf{i}_{\text{bus}} \tag{1}$$

$$\mathbf{v}_{\text{bus}} + \Delta\mathbf{v}_{\text{bus}} = (\mathbf{Y}_{\text{bus}} + \Delta\mathbf{Y}_{\text{bus}})^{-1}\mathbf{i}_{\text{bus}} \tag{2}$$

$$\mathbf{v}_{\text{bus}} + \Delta\mathbf{v}_{\text{bus}} = \mathbf{Y}_{\text{bus}}^{-1}(\mathbf{i}_{\text{bus}} + \Delta\mathbf{i}_{\text{bus}}) \tag{3}$$

$$\Delta\mathbf{i}_{\text{bus}} = \mathbf{Y}_{\text{bus}}((\mathbf{Y}_{\text{bus}} + \Delta\mathbf{Y}_{\text{bus}})^{-1} - \mathbf{Y}_{\text{bus}}^{-1})\mathbf{i}_{\text{bus}} \tag{4}$$

In the compensation current method, compensation currents $\Delta\mathbf{i}_{\text{bus}}$ are defined such that their injection in the original network leads to $(\mathbf{v}_{\text{bus}} + \Delta\mathbf{v}_{\text{bus}})$ as shown in Fig. 1c and given by (3). This approach is categorized as pre-compensation method discussed in [16]. The term $\mathbf{Y}_{\text{bus}}^{-1}$ is same in (3) and (1), which suggest no need to recalculate the bus impedance matrix. Then, $\Delta\mathbf{i}_{\text{bus}}$ is given as (4) which is obtained by equating (2) with (3). The following discussion is dedicated to calculate $\Delta\mathbf{i}_{\text{bus}}$ with minimum computational effort.

$$\Delta\mathbf{Y} = \begin{bmatrix} \Delta\mathbf{Y}_{\text{fcl}} & -\Delta\mathbf{Y}_{\text{fcl}} & \mathbf{0} \\ -\Delta\mathbf{Y}_{\text{fcl}} & \Delta\mathbf{Y}_{\text{fcl}} & \mathbf{0} \\ \mathbf{0} & \mathbf{0} & \mathbf{Y}_{\text{f}} \end{bmatrix} \in \mathbb{C}^{9\times 9} \tag{5}$$

$$(\mathbf{A}+\mathbf{U}\mathbf{V}^{\text{T}})^{-1} = \mathbf{A}^{-1} - \mathbf{A}^{-1}\mathbf{U}(\mathbf{I} + \mathbf{V}^{\text{T}}\mathbf{A}^{-1}\mathbf{U})^{-1}\mathbf{V}^{\text{T}}\mathbf{A}^{-1} \tag{6}$$

$$\begin{bmatrix}\Delta\mathbf{i}_g \\ \Delta\mathbf{i}_h\end{bmatrix} = -\begin{bmatrix}\mathbf{0} \\ \mathbf{I}_9\end{bmatrix}(\mathbf{I}_{3n} + \begin{bmatrix}\mathbf{0} & \Delta\mathbf{Y}\end{bmatrix}\begin{bmatrix}\mathbf{Z}_{gg} & \mathbf{Z}_{gh} \\ \mathbf{Z}_{hg} & \mathbf{Z}_{hh}\end{bmatrix}\begin{bmatrix}\mathbf{0} \\ \mathbf{I}_9\end{bmatrix})^{-1} \cdot \begin{bmatrix}\mathbf{0} & \Delta\mathbf{Y}\end{bmatrix}\begin{bmatrix}\mathbf{v}_g \\ \mathbf{v}_h\end{bmatrix} \tag{7}$$

Matrix $\Delta\mathbf{Y}_{\text{bus}}$ is sparse with elements corresponding to $\Delta\mathbf{Y}_{\text{fcl}}$ and $\mathbf{Y}_{\text{f}}$ at buses $\{r, s, k\}$. Matrix $\Delta\mathbf{Y}_{\text{bus}}$ is given as $[\mathbf{0}, \mathbf{0}; \mathbf{0}, \Delta\mathbf{Y}]$ which can be considered as small perturbation in $\mathbf{Y}_{\text{bus}}$, where $\Delta\mathbf{Y}$ defined by (5) is a block matrix corresponding to buses $\{r, s, k\}$. The Woodbury matrix identity (6) gives the inverse of matrix $\mathbf{A}$ with perturbation $\mathbf{U}\mathbf{V}^{\text{T}}$. Using this identity, the term $(\mathbf{Y}_{\text{bus}} + \Delta\mathbf{Y}_{\text{bus}})^{-1}$ in (4) is obtained by substituting $\mathbf{A} = \mathbf{Y}_{\text{bus}}$, $\mathbf{U} = [\mathbf{0}, \mathbf{I}_9]^{\text{T}}$ and $\mathbf{V} = [\mathbf{0}, \Delta\mathbf{Y}]^{\text{T}}$ in (6) with $\mathbf{I}_9 \in \mathbb{U}^{9\times 9}$. Eq. (4) is substituted with $(\mathbf{Y}_{\text{bus}} + \Delta\mathbf{Y}_{\text{bus}})^{-1}$ and is rewritten in block matrix form as (7) for two sets of buses which are $h = \{r, s, k\}$ and g representing set of remaining system buses, where $\mathbf{Z}_{gg}$, $\mathbf{Z}_{gh}$, $\mathbf{Z}_{hg}$, and $\mathbf{Z}_{hh}$ are blocks of the bus impedance matrix given by $\mathbf{Y}_{\text{bus}}^{-1}$.

Solving (7) for $\Delta\mathbf{i}_h \in \mathbb{C}^9$ leads to the expression of compensation currents given by (8). The terms $\mathbf{v}_h \in \mathbb{C}^9$ and $\mathbf{Z}_{hh} \in \mathbb{C}^{9\times 9}$ are blocks of $\mathbf{v}_{\text{bus}}$ and $\mathbf{Y}_{\text{bus}}^{-1}$ corresponding to buses $\{r, s, k\}$, respectively. Matrix $\Delta\mathbf{Y}$ accounts for sequence network coupling introduced due to $\Delta\mathbf{Y}_{\text{fcl}}$ and $\mathbf{Y}_{\text{f}}$. The compensation current $\Delta\mathbf{i}_h$ evaluation requires solving system of 9 linear equations. After obtaining $\Delta\mathbf{i}_h$, the solution of faulted system with the FCL is obtained using (3).

$$\Delta\mathbf{i}_h = -(\mathbf{I}_9 + \Delta\mathbf{Y}\mathbf{Z}_{hh})^{-1}\Delta\mathbf{Y}\mathbf{v}_h, \text{ where,} \tag{8}$$

$$\Delta\mathbf{i}_h = \begin{bmatrix}\Delta\mathbf{i}_r \\ \Delta\mathbf{i}_s \\ \Delta\mathbf{i}_k\end{bmatrix}, \mathbf{Z}_{hh} = \begin{bmatrix}\mathbf{Z}_{rr} & \mathbf{Z}_{rs} & \mathbf{Z}_{rk} \\ \mathbf{Z}_{sr} & \mathbf{Z}_{ss} & \mathbf{Z}_{sk} \\ \mathbf{Z}_{kr} & \mathbf{Z}_{ks} & \mathbf{Z}_{kk}\end{bmatrix}, \text{ and } \mathbf{v}_h = \begin{bmatrix}\mathbf{v}_r \\ \mathbf{v}_s \\ \mathbf{v}_k\end{bmatrix}$$

$$\mathbf{v}_{\text{bus}}^e + \Delta\mathbf{v}_{\text{bus}}^e = (\mathbf{Y}_{\text{bus}}^e)^{-1}(\mathbf{i}_{\text{bus}}^e + \begin{bmatrix}\mathbf{0} \\ \Delta\mathbf{i}_h^e\end{bmatrix}), \forall e \in \{00, 01, 02\} \tag{9}$$

Furthermore, after calculation of $\Delta\mathbf{i}_h$ the sequence networks can be solved individually for symmetrical systems with $\mathbf{Y}_{\text{bus}} = \text{diag}(\mathbf{Y}_{\text{bus}}^{00}, \mathbf{Y}_{\text{bus}}^{01}, \mathbf{Y}_{\text{bus}}^{02})$. For example, positive sequence network (e = 01) is solved using (9) with compensation current $\Delta\mathbf{i}_h^{01} = [\Delta I_r^{01}, \Delta I_s^{01}, \Delta I_k^{01}]^{\text{T}}$. Similarly, the zero ($e$ = 00) and negative sequence (e = 02) networks can be solved. Eq. (9) shows that the method can be applied in decoupled fashion. The proposed method has following features:

- It eliminates need for recalculation of the modified bus impedance matrix $(\mathbf{Y}_{\text{bus}} + \Delta\mathbf{Y}_{\text{bus}})^{-1}$ irrespective of fault location, fault type or FCL impedance change.
- It requires less computations to obtain $\Delta\mathbf{v}_{\text{bus}}$ by solving (8) of 9 linear equations as compared to solving (2) of $3n$ linear equations, for a case of FCL impedance change.
- It enables solving the sequence networks in decoupled fashion with (9) irrespective of coupling in $\Delta\mathbf{Y}$ due to fault type or FCL activation.

III. Validation with Time-domain Simulations

This section validates the proposed method by comparing its results with those obtained using time-domain simulation consisting detailed model of an FCL. For this purpose, various test cases are defined for a test system.

A. Test System and Test Cases

Fig. 3 shows the single line diagram of the test system considered for time-domain simulations. The test system consists

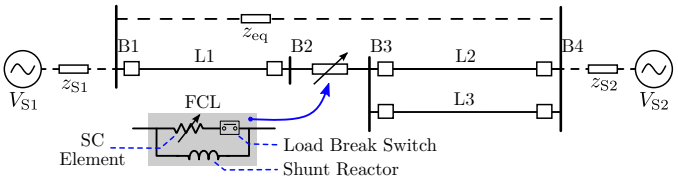

Fig. 3. Single line diagram of test system with FCL.

TABLE II
TEST SYSTEM DATA.

Element	Parameters
Source 1	138 kV, $V_{S1}=1.0085\angle 42.45°$ pu, $z_{S1}^{00}=0.144+j3.857\ \Omega$, $z_{S1}^{01}=z_{S1}^{02}=0.492+j5.059\ \Omega$.
Source 2	138 kV, $V_{S2}=0.9594\angle 16.82°$ pu, $z_{S2}^{00}=0.287+j8.548\ \Omega$, $z_{S2}^{01}=z_{S2}^{02}=1.626+j30.346\ \Omega$.
Equivalent	$z_{eq}^{00}=51.043+j671.222\ \Omega$, $z_{eq}^{01}=z_{eq}^{02}=7.86+j49.743\ \Omega$.
Line 1-3	$z_{L}^{00}=0.49+j9.74\ \Omega$, $z_{L}^{01}=z_{L}^{02}=0.54+j4.55\ \Omega$.
SCFCL	$I_{cri}=2.5$ kA, $z^{li}=0.1\ \Omega$, $z^{hi}=j10\ \Omega$.

of four buses B1-B4 and three transmission lines L1-L3 at 138 kV. The impedances z_{S1}, z_{S2}, and z_{eq} are obtained using short circuit equivalent of IEEE 118 bus system [18] across buses 100 (B1) and 106 (B4). Table II presents the parameter data for all test system elements. An FCL is considered between buses B2 and B3.

This study considers a resistive superconducting fault current limiter with construction as shown in Fig. 3. Each phase of the FCL consists of a superconducting (SC) element, a series load break switch and a shunt reactor [8], [9]. In normal condition, the SC element remains in superconducting state providing negligible impedance. During fault, the resistance of the SC element increases for currents higher than critical current value (I_{cri}) leading current commutation to shunt reactor. The series load break switch disconnects the quenched SC element for predefined time period to ensure its successful recovery to superconducting state. Meanwhile the shunt reactor remains in the network and provides current limiting impedance [9]. Table II presents the FCL parameters.

For the time-domain simulations, the SC element is modeled using the E-J power law for YBCO superconductors [19]. The operation of the load break switch is controlled using an input from the SC element of the corresponding phase [20]. The time-domain simulations are carried out using EMTP-ATP and direct Fourier transform (DFT) based phasor estimation is employed to measure FCL current and bus voltages. Table III presents the test cases considered for the time-domain study. Case 1 considers a single line to ground (SLG) fault at bus B4, and Case 2 considers line-line (LL) fault at bus B4. Case 1 and 2 consider the critical current rating of the FCL to be 2.5 kA. Case 3 consider an SLG fault at bus B4 with critical current rating of 1.5 kA which is included to demonstrate effect of change in critical current rating on FCL activation.

For each test case, the phasors calculated using the proposed method are validated with those obtained using time-domain simulations. In the simulations, the phasors are estimated

TABLE III
TEST CASES FOR TIME-DOMAIN SIMULATION STUDY.

Cases	Fault type	Fault Bus	I_{cri} (kA)
Case 1	SLG	B4	2.5
Case 2	LL	B4	2.5
Case 3	SLG	B4	1.5

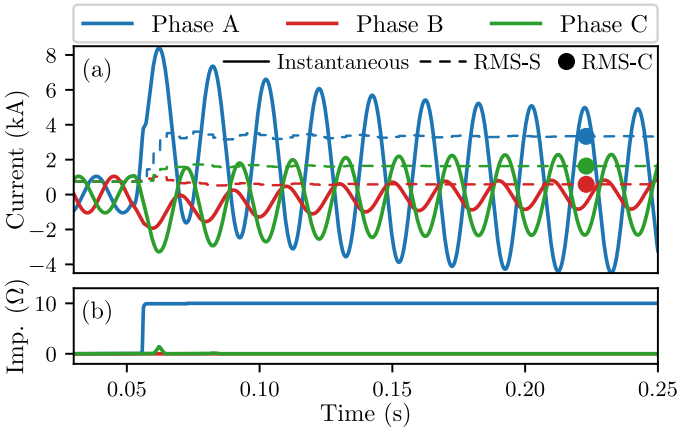

Fig. 4. Time-domain simulation results for Case 1: (a) FCL currents showing instantaneous value, rms value of estimated phasor (RMS-S), and analytically calculated rms value (RMS-C); and (b) FCL impedance magnitudes.

from the corresponding instantaneous quantities using DFT. After reaching the steady state in time-domain simulations, the values of these simulated phasors are compared with respective calculated phasors. For visualization purposes, Fig. 4-6 show the rms values of phasors obtained from simulations (RMS-S) and those obtained using analytical calculations (RMS-C) for Cases 1-3, respectively.

B. Case 1

1) Time-domain simulation: The SLG fault involving phase A is simulated at 0.054 s with fault resistance of 10 $\mu\Omega$. Fig. 4a shows the phase currents flowing through the FCL and Fig. 4b shows the FCL phase impedance magnitude.

After fault inception, Fig. 4a shows an increase in phase A current beyond FCL critical current leading to SC element quenching. The FCL impedance transitions to high impedance state in 2-3 ms as shown in Fig. 4b. The load break switch in phase A disconnects the SC element at 0.0725 s after which the shunt reactor of phase A carries the FCL current and provides necessary current limiting impedance. The SC elements in phases B and C remain in superconducting state and FCL provide low impedance in these phases as shown in Fig. 4b. After one cycle from fault inception, the FCL impedance appears as $\mathbf{Z}_{fcl}^{abc} = \text{diag}(j10, 0.1, 0.1)\ \Omega$. Fig. 4a also shows the rms value of estimated FCL current phasors. The estimated phasors after transient are given as $\mathbf{i}_{fcl}^{abc} = [3334.22\angle -44.00°; 587.82\angle -179.12°; 1632.95\angle 136.11°]$ A. Similarly, the phasors of bus voltages are estimated and converted to sequence domain. Table IV lists these bus voltages for Case 1.

2) Analytical calculation: Case 1 is solved using (9). The values of $\mathbf{v}_{bus}^{e}$, $\mathbf{i}_{bus}^{e}$ and $\mathbf{Y}_{bus}^{e}$ are obtained from pre-fault

TABLE IV
BUS VOLTAGES OBTAINED WITH DIFFERENT METHODS FOR CASE 1.

	Bus	EMTP Simulation (V)	Analytical Calculations (V)
V^{00}	B1	$1834.25\angle -153.29°$	$1834.30\angle -153.31°$
	B2	$6223.80\angle -154.38°$	$6224.06\angle -154.39°$
	B3	$17063.14\angle -141.07°$	$17063.60\angle -141.07°$
	B4	$19202.33\angle -142.63°$	$19202.67\angle -142.63°$
V^{01}	B1	$70123.04\angle\ 040.58°$	$70122.99\angle\ 040.58°$
	B2	$62901.06\angle\ 038.98°$	$62900.85\angle\ 038.98°$
	B3	$51839.43\angle\ 037.53°$	$51839.72\angle\ 037.53°$
	B4	$48279.99\angle\ 036.25°$	$48280.25\angle\ 036.25°$
V^{02}	B1	$8929.56\angle -148.69°$	$8929.76\angle -148.70°$
	B2	$15166.64\angle -150.34°$	$15167.08\angle -150.34°$
	B3	$25996.56\angle -143.50°$	$25996.32\angle -143.50°$
	B4	$29083.75\angle -144.48°$	$29083.60\angle -144.48°$

TABLE V
ERROR IN BUS VOLTAGES BETWEEN EMTP AND ANALYTICAL RESULTS.

	Case 1	Case 2	Case 3
Maximum magnitude error	0.0041%	0.0069%	0.0030%
Maximum angle difference	0.0146°	0.0130°	0.0081°

condition. For Case 1, the external branch admittances are given as $\Delta\mathbf{Y}_{\text{fcl}}^{\text{abc}} = \text{diag}(\Delta y, 0, 0)$ and $\mathbf{Y}_{\text{f}}^{\text{abc}} = \text{diag}(\frac{1}{R_{\text{f}}}, 0, 0)$ with $\Delta y = (\frac{1}{j10} - \frac{1}{0.1})$ S and $R_{\text{f}} = 10\ \mu\Omega$. These branch admittances are converted to sequence domain and substituted in (8) to obtain the compensation currents $\Delta\mathbf{i}_h^e$. Then, the modified bus voltages are obtained using (9) with $\Delta\mathbf{i}_h^e$. Table IV lists the calculated bus voltages in sequence domain during fault. The FCL current is obtained from bus voltages and is given as $\mathbf{i}_{\text{fcl}}^{\text{abc}} = [3334.14\angle -43.99°; 587.80\angle -179.13°; 1632.91\angle 136.07°]$ A. Fig. 4a shows the rms values of calculated FCL current with a dot, which match with those obtained using simulations. A comparison between the bus voltages presented in Table IV shows that the calculated bus voltages matches the simulation results with maximum magnitude error of 0.0041% and maximum angle difference of $0.0146°$, as mentioned in Table V.

C. Case 2

1) Time-domain simulation: The LL fault involving phases B and C is simulated at 0.054 s with fault resistance of $10\ \mu\Omega$. Fig. 5a and 5b show FCL current and impedance for all phases. Fig. 5a shows increase in phases B and C beyond critical current, which leads to FCL activation in these phases as shown in Fig. 5b. In phase A, the FCL remains in low impedance state. After a cycle in fault, the FCL impedance appears as $\mathbf{Z}_{\text{fcl}}^{\text{abc}} = \text{diag}(0.1, j10, j10)\ \Omega$. The rms values of estimated FCL phase current are shown on Fig. 5a, and after transient is given as $\mathbf{i}_{\text{fcl}}^{\text{abc}} = [744.06\angle 26.96°; 3203.16\angle -136.05°; 2692.33\angle 47.50°]$ A. An addition of FCL phase currents gives neutral current of $202.13\angle 29.34°$ A, which suggests flow of zero sequence currents in network for Case 2. Furthermore, the estimated bus voltages give zero sequence voltages of $255.36\angle -62.84°$, $912.42\angle -63.35°$, $894.36\angle 117.04°$ and $565.85\angle 117.37°$ V at buses B1, B2, B3 and B4, respectively. These voltages have phase shift of

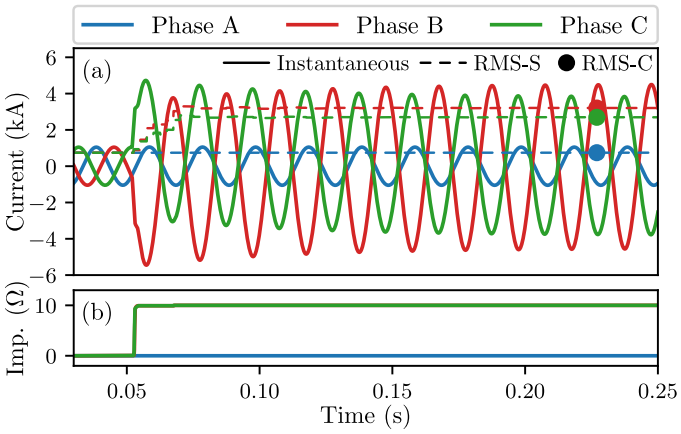

Fig. 5. Time-domain simulation results for Case 2: (a) FCL currents showing instantaneous value, rms value of estimated phasor (RMS-S), and analytically calculated rms value (RMS-C); and (b) FCL impedance magnitudes.

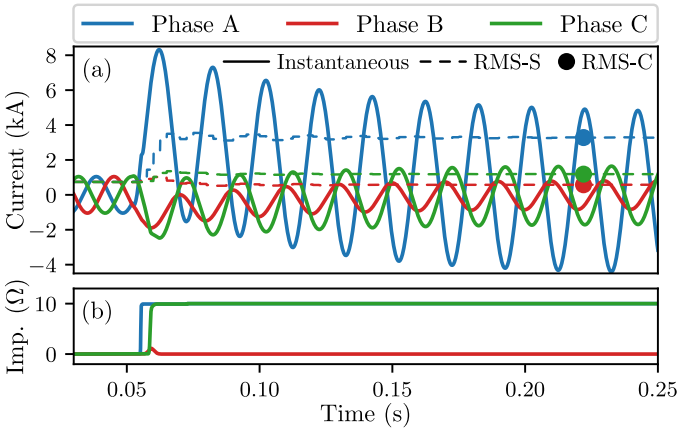

Fig. 6. Time-domain simulation results for Case 3: (a) FCL currents showing instantaneous value, rms value of estimated phasor (RMS-S), and analytically calculated rms value (RMS-C); and (b) FCL impedance magnitudes.

$\approx 180°$ across the FCL buses indicating voltage reversal across the FCL buses in zero sequence network.

2) Analytical calculation: For Case 2, the external branch admittances are given as $\Delta\mathbf{Y}_{\text{fcl}}^{\text{abc}} = \text{diag}(0, \Delta y, \Delta y)$ and $\mathbf{Y}_{\text{f}}^{\text{abc}} = \frac{1}{R_{\text{f}}}[0, 0, 0; 0, 1, -1; 0, -1, 1]$. The bus voltages during fault are calculated using (8)-(9) as discussed for Case 1. Their comparison with simulation gives maximum magnitude error of 0.0069% and maximum angle difference of $0.013°$ as seen in Table V. The rms values of calculated FCL current is given as $\mathbf{i}_{\text{fcl}}^{\text{abc}} = [744.03\angle 26.96°; 3203.18\angle -136.06°; 2692.37\angle 47.49°]$ A, which matches with the simulation results as shown in Fig. 5a. The analytical calculation confirms the voltage reversal across the FCL buses in zero sequence network.

D. Case 3

1) Time-domain simulation: The simulations for Case 1 is repeated for Case 3 with one modification of $I_{\text{cri}} = 1.5$ kA. Fig. 6a and 6b show FCL current and impedance for all phases. The FCL activates in faulted phase A due to increase in current. In addition, the lower value of I_{cri} also leads to FCL

activation in phase C for an increase in phase C current due to coupling between phase impedances of the system equipment. As seen in Fig. 6b, the lower value of critical current rating leads to FCL activation in both faulty phase A and healthy phase C. Such case of FCL activation in healthy phases is termed as inconsistent FCL activation for further discussions. The FCL impedance appears as $\mathbf{Z}_{\text{fcl}}^{\text{abc}} = \text{diag}(j10, 0.1, j10)\ \Omega$ after one cycle in fault. Fig. 6a shows the rms values of estimated the FCL current phasors, which are given as $\mathbf{i}_{\text{fcl}}^{\text{abc}} = [3283.12\angle -44.13°; 578.83\angle -177.09°; 1186.09\angle 134.57°]$ A.

2) Analytical calculation: For Case 3, the external branch admittances are given as $\Delta\mathbf{Y}_{\text{fcl}}^{\text{abc}} = \text{diag}(\Delta y, 0, \Delta y)$ and $\mathbf{Y}_{\text{f}}^{\text{abc}} = \text{diag}(\frac{1}{R_{\text{f}}}, 0, 0)$. Table V shows the maximum magnitude error of 0.0030% and maximum angle error of $0.0081°$ in calculated bus voltages. The rms values of calculated FCL current is given as $\mathbf{i}_{\text{fcl}}^{\text{abc}} = [3282.85\angle -44.14°; 578.83\angle -177.10°; 1186.09\angle 134.56°]$ A, which matches with the simulation results as shown in Fig. 6a.

E. Discussions

Following points summarize the results of the test cases:

- For the same fault, Case 1 observes FCL activation consistent with the fault type in contrast to Case 3 with inconsistent FCL activation. Furthermore, it is possible for the FCL to activate in healthy phases for lower critical current. Such situations of consistent and inconsistent FCL activation for any fault type can be analyzed using the proposed method, since the branches $\Delta\mathbf{Y}_{\text{fcl}}$ and $\mathbf{Y}_{\text{f}}$ are modeled individually in (8) while calculating $\Delta\mathbf{i}_h$.
- Case 2 observed flow of neutral current during the LL fault, which is generally not the case for systems without FCL. In Case 2, the fault leads to two-phase activation of the FCL. This FCL activation introduces interconnection to the zero sequence network as shown in Fig. 2c. This interconnection causes flow of zero sequence currents in the network and zero sequence voltage reversal across FCL buses. This result reaffirms the interconnection defined in Fig. 2b-c which suggest that the zero sequence currents can flow during single-phase or two-phase FCL activation irrespective of fault type.
- The proposed method reproduces the steady state values of the time-domain simulation results within acceptable error limits as listed in Table V. The errors are attributed to the approximations in time-domain modeling.
- The steady state short circuit solution obtained using the proposed method is useful to analyze the performance of protection relays based on phasor quantities. In addition, the calculated steady state values can be used to obtain transient components of the fault current using standards, such as IEC 60909.

IV. Application to Large Power Systems and Computational Effort

This section presents an application of the proposed method to a large power system. The aim here is to find the change in bus fault currents in IEEE 118 bus system after an FCL installation. Furthermore, the computational effort of the proposed method is compared with a coupled method.

TABLE VI
Computational effort comparison of analysis methods.

Task	Number of times task performed			
	Proposed		Coupled	
	count	size	count	size
Initialization				
(a) $\mathbf{Y}_{\text{bus}}$ formulation	3	$\mathbb{C}^{n\times n}$	1	$\mathbb{C}^{3n\times 3n}$
(b) $\mathbf{Z}_{\text{bus}}$ vector calculation	6	$\mathbb{C}^{n}$	0	
For m cases per bus				
(c) $\mathbf{Y}_{\text{bus}}$ update	0		m	$\mathbb{C}^{3n\times 3n}$
(d) $\mathbf{Z}_{\text{bus}}$ vector calculation	3	$\mathbb{C}^{n}$	$3m$	$\mathbb{C}^{3n}$
(e) Solution of linear equations	m	$\mathbb{C}^{9\times 9}$	m	$\mathbb{C}^{3\times 3}$

A. Method Description and Their Computational Effort

Here, the computational effort required by each method is discussed to obtain fault currents at various buses. The computational effort is divided into various tasks (a)-(e) as shown in Table VI and compared with number of times a task is performed and dimension of corresponding coefficient matrix. Following discussion considers that the fault current at a bus need to be calculated for m different cases of $\Delta\mathbf{Y}$, which may consists of different fault types, fault resistances and FCL activation types. The methods are provided with bus admittance matrices rather than bus impedance matrices, since the former are sparse for large power systems. Then, the required $\mathbf{Z}_{\text{bus}}$ vector is calculated from corresponding $\mathbf{Y}_{\text{bus}}$ using the LU factorization and forward-backward substitutions.

1) Proposed Method: In initialization, the bus admittance matrices are formulated with $\mathbf{Y}_{\text{fcl}}$ at FCL buses. Task (a) is performed 3 times to obtain $\mathbf{Y}_{\text{bus}}^{00}, \mathbf{Y}_{\text{bus}}^{01}, \mathbf{Y}_{\text{bus}}^{02} \in \mathbb{C}^{n\times n}$ which are required in (9). Eq. (8) requires bus impedance matrix elements corresponding to FCL buses, which are same for all faults in the system. These are obtained from $\mathbf{Z}_{\text{bus}}$ vectors corresponding to two FCL buses and three sequence networks. Hence, task (b) is performed 6 times to obtain $\mathbf{Z}_{\text{bus}}$ vectors with n elements.

For each case, the method does not require modifying the original bus admittance matrices. Hence, task (c) is not performed in this method. To obtain the bus impedance matrix elements corresponding to faulted bus in (8), task (d) is performed 3 times for each sequence network. Thereafter, the compensation currents are obtained by solving system of 9 linear equations which is shown as task (e) in Table VI. To analyze m cases of $\Delta\mathbf{Y}$ on a same faulted bus, task (e) is performed for m times by modifying $\Delta\mathbf{Y}$. Then, the network solution is obtained by substituting in compensation currents in (9).

2) Coupled Method: In this method, the faulted system is solved for three sequence networks simultaneously. This method modifies the bus admittance matrix $\mathbf{Y}_{\text{bus}}$ with $\Delta\mathbf{Y}_{\text{fcl}}$ and fault currents are calculated for $\mathbf{Y}_{\text{f}}$ using classical fault analysis method. Task (a) is performed once to formulate

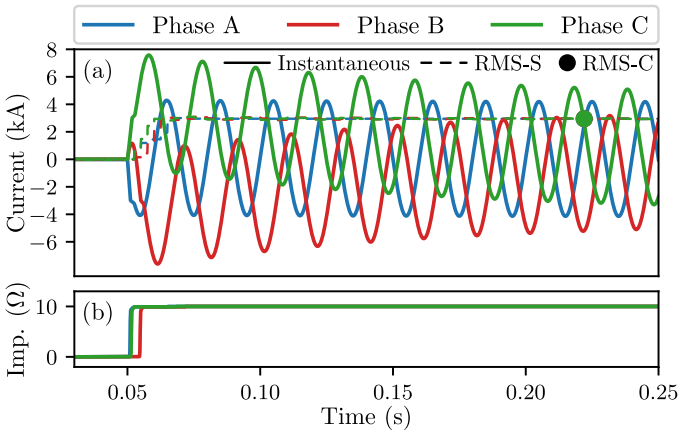

Fig. 7. Time-domain simulation results for a three-line fault at bus 94 in IEEE 118 bus system: (a) FCL currents showing instantaneous value, rms value of estimated phasor (RMS-S), and analytically calculated rms value (RMS-C); and (b) FCL impedance magnitudes.

original $\mathbf{Y}_{\text{bus}} \in \mathbb{C}^{3n\times 3n}$. Task (b) is not performed for this method.

For a given value of FCL impedance, the $\mathbf{Y}_{\text{bus}}$ is modified with $\Delta\mathbf{Y}_{\text{fcl}}$ at FCL buses which represents task (c). Then, the bus impedance matrix elements corresponding to faulted bus is obtained from 3 bus impedance vectors which represents task (d). Later, the fault current is calculated for $\mathbf{Y}_{\text{f}}$ which represents task (e). For m cases of $\Delta\mathbf{Y}$, tasks (c) and (e) are performed m times and task (d) is performed $3m$ times.

B. Fault Analysis of IEEE 118 Bus System

The IEEE 118 bus system is considered for the fault analysis. The system contains 177 transmission lines at 345 kV and 138 kV. The two voltage levels are connected with nine-three winding transformers. The system data is obtained from [18]. For the analysis, the synchronous machines are converted to Norton equivalents and load are converted to constant shunt impedances. An FCL is proposed to limit fault currents at bus 100 by splitting the bus. Bus 100 is split into 100A and 100B such that the transmission lines connected to buses 094, 099 and 104 are connected to 100B and rest of the components are connected to 100A. Then, the FCL is connected between buses 100A and 100B. The FCL parameters considered for this study are $I_{\text{cri}} = 2$ kA, $z^{\text{li}} = j0.1$ mΩ, and $z^{\text{hi}} = j10$ Ω.

Before discussing the fault analysis, the result of the proposed method for a fault is compared with the time-domain simulation result. For this purpose, IEEE 118 bus system with the FCL is modeled in EMTP-ATP, and a three-line fault is considered at bus 94 with no-load condition. Fig. 7a shows the FCL current and impedance for all phases. The fault is simulated at $t = 0.5$ s, which leads to an increase in the FCL current. This current increases in FCL impedance in all phases, as shown in Fig. 7b, after which the FCL impedance appears as $\mathbf{Z}^{\text{abc}}_{\text{fcl}} = \text{diag}(j10, j10, j10)$ Ω. Fig. 7a shows the rms value of the estimated FCL current phasors, which are given as $\mathbf{i}^{\text{abc}}_{\text{fcl}} = [2950.83\angle -89.35°; 2950.49\angle 150.65°; 2950.89\angle 30.66°]$ A. To obtain network solution with the proposed method, the external branch admittances of $\Delta\mathbf{Y}^{\text{abc}}_{\text{fcl}} = \Delta y\,\text{diag}(1,1,1)$ and $\mathbf{Y}^{\text{abc}}_{\text{f}} = \frac{1}{R_{\text{f}}}\text{diag}(1,1,1)$ are considered. The calculated FCL current is given as $\mathbf{i}^{\text{abc}}_{\text{fcl}} = [2937.35\angle -89.37°; 2937.35\angle 150.63°; 2937.35\angle 30.63°]$ A, and the respective rms values are shown in Fig. 7a. The simulated FCL current matches the calculated FCL current with maximum error of 0.5%, which is due to modeling differences. Repeating this validation exercise is time consuming and may not be necessary. Hence, the results of the proposed method are validated with those of the coupled method in following discussions.

TABLE VII
TOTAL CPU EXECUTION TIME (IN SECONDS).

Analyzed Cases	Proposed	Coupled
70 ($I_{\text{cri}} = 2$ kA)	0.0304	0.2295
115 ($I_{\text{cri}} = 1$ kA)	0.0492	0.3741

For fault analysis, four types of faults are considered at 119 buses which includes SLG, LL, double-line to ground and three-line faults. Among all these fault cases, only the cases leading to FCL activation are analyzed using previously discussed methods. These cases are identified by evaluating the FCL current during the fault. The FCL current is evaluated using classical fault analysis method by considering the FCL in low impedance state. This analysis assumes that the FCL activates in a phase if its rms current is higher than $\frac{I_{\text{cri}}}{2\sqrt{2}}$ [21].

A total of 476 bus faults are considered for this study. The FCL with critical current rating of $I_{\text{cri}} = 2$ kA activates for 70 fault cases. These cases includes 64 cases of consistent and 6 cases of inconsistent FCL activation. The fault currents for system with FCL are calculated using both of the previously discussed methods. The result shows that buses 95-103 and 105 observe reduction in bus fault currents due to FCL installation, where the maximum fault current reduction of 19% is observed at Bus 100A. The fault currents calculated using both methods matches each other with maximum magnitude error of 0.00004%. In addition, these calculations are repeated for FCL with $I_{\text{cri}} = 1$ kA. This FCL activated for 115 fault cases comprising 95 consistent and 10 inconsistent cases, suggesting lower I_{cri} causes FCL activation for faults at more buses.

The methods are executed on same personal computer to measure their CPU time. Table VII gives the CPU time taken by both the methods. For FCL with $I_{\text{cri}} = 2$ kA, the execution time taken by the proposed method is 0.0304 s compared to 0.2295 s by the coupled method. Similarly, the execution time taken by proposed method and coupled method is 0.0492 s and 0.3741 s, respectively for FCL with $I_{\text{cri}} = 1$ kA. This result shows that the proposed method is faster than the coupled method.

C. Extension to Power Systems with Multiple FCLs

The proposed compensation current method is extended for analysis of system with two FCLs. Here, the fault currents need to be calculated considering impedance change of two FCLs. In this case, the external branches are introduced

at 5 system buses and their admittance $\Delta\mathbf{Y} \in \mathbb{C}^{15\times15}$ is given by (10). Matrices $\Delta\mathbf{Y}_{\text{fcl1}}$ and $\Delta\mathbf{Y}_{\text{fcl2}}$ account for the admittance changes in FCL 1 and FCL 2, respectively. Then, the compensation currents $\Delta\mathbf{i}_h \in \mathbb{C}^{15}$ are calculated at buses in set h consisting four FCL buses and a fault bus using (8) with $\mathbf{Z}_{hh} \in \mathbb{C}^{15\times15}$.

$$\Delta\mathbf{Y} = \begin{bmatrix} \Delta\mathbf{Y}_{\text{fcl1}} & -\Delta\mathbf{Y}_{\text{fcl1}} & 0 & 0 & 0 \\ -\Delta\mathbf{Y}_{\text{fcl1}} & \Delta\mathbf{Y}_{\text{fcl1}} & 0 & 0 & 0 \\ 0 & 0 & \Delta\mathbf{Y}_{\text{fcl2}} & -\Delta\mathbf{Y}_{\text{fcl2}} & 0 \\ 0 & 0 & -\Delta\mathbf{Y}_{\text{fcl2}} & \Delta\mathbf{Y}_{\text{fcl2}} & 0 \\ 0 & 0 & 0 & 0 & \mathbf{Y}_{\text{f}} \end{bmatrix} \tag{10}$$

For demonstration, another FCL with $z^{\text{hi}} = j10\ \Omega$ is added in series with branch between buses 099 and 100B of IEEE 118 bus system discussed earlier. An SLG fault at bus 106 is analyzed with single-phase activation of both FCLs using both methods. For this analysis using proposed method, task (b) in Table VI need to be performed 12 times for four FCL buses and task (e) requires solving system of 15 linear equations. However, the tasks of coupled method remains the same as mentioned in Table VI. The calculated fault current in phase domain is given as $[11.673\angle-41.10°, 0, 0]$ kA. The result of proposed method matches the results of the coupled method with an error of 0.00002%. The compensation current calculation require solving system of 9 and 15 linear equations for system with 1 and 2 FCLs, respectively. Similarly, the proposed method can be extended to a system with f number of FCLs where the evaluation of compensation current requires solving system of $3(1+2f)$ linear equations.

D. Future Study

This study dealt with FCLs which have constant impedance z^{hi} after activation. However, there are some FCLs which present non-linear impedance after activation, such as saturated iron core superconducting FCL. The application of proposed method to analyze the power systems with such FCLs is not presented in this paper due to space constraint. This topic will be considered in the future.

V. Conclusion

This paper proposes a fault analysis method for systems with FCL. The proposed method solves the three sequence networks individually with compensation currents compared to solving them simultaneously due to coupling introduced by FCL impedance. The proposed method is computationally efficient for analyzing large power systems. The proposed method does not require the recalculation of bus impedance matrices for a change in the FCL impedance. For a faulted system consisting of f number of FCLs, the proposed method requires solving $3(1+2f)$ linear equations to obtain compensation currents. The single-phase or two-phase FCL activation during phase faults leads to the flow of neutral currents, which are defined by respective sequence network interconnections.

References

[1] G. Declercq, M. El-Adnani *et al.*, "The mechanical effects of short circuit curretns in open air substations (Part II)," CIGRE Working Group 23.03, Techn. Brochure 214, Oct. 2002.

[2] H. Schmitt, J. A. Filho *et al.*, "Guideline on the impacts of fault current limiting devices on protection systems," CIGRE Working Group A3.16, Tech. Brochure 339, Feb. 2008.

[3] S. Kodle, V. Padmini *et al.*, "Application of super conducting fault current limiter in indian grid," in *IEEE 6th International Conference on Power Systems (ICPS)*. IEEE, 2016, pp. 1–6.

[4] W. T. B. de Sousa, D. Kottonau *et al.*, "Deployment of a resistive superconducting fault current limiter for improvement of voltage quality and transient recovery voltage," *IEEE Transactions on Applied Superconductivity*, vol. 31, no. 1, pp. 1–9, 2020.

[5] R. Silva, G. Mafra *et al.*, "Impact of superconducting fault current limiters on delayed current zeros in industrial power systems," *International Journal of Electrical Power & Energy Systems*, vol. 145, p. 108594, 2023.

[6] M. E. Elshiekh, D.-E. A. Mansour, and A. M. Azmy, "Improving fault ride-through capability of dfig-based wind turbine using superconducting fault current limiter," *IEEE transactions on Applied Superconductivity*, vol. 23, no. 3, pp. 5 601 204–5 601 204, 2012.

[7] S. Seo, S.-J. Kim *et al.*, "A hybrid superconducting fault current limiter for enhancing transient stability in korean power systems," *Physica C: Superconductivity*, vol. 494, pp. 331–334, 2013.

[8] M. Moyzykh, D. Gorbunova *et al.*, "First Russian 220 kV superconducting fault current limiter (SFCL) for application in city grid," *IEEE Transactions on Applied Superconductivity*, vol. 31, no. 5, pp. 1–7, 2021.

[9] P. Tixador, *Superconducting Fault Current Limiter: Innovation for the Electric Grids*. World Scientific, 2018.

[10] P. M. Anderson, *Analysis of faulted power systems*. John Wiley & Sons, 1995, vol. 11.

[11] R. K. Gajbhiye, B. Gopi *et al.*, "Computationally efficient methodology for analysis of faulted power systems with series-compensated transmission lines: A phase coordinate approach," *IEEE Transactions on Power Delivery*, vol. 23, no. 2, pp. 873–880, 2008.

[12] J. Song, M. Cheah-Mane *et al.*, "Short-circuit analysis of grid-connected pv power plants considering inverter limits," *International Journal of Electrical Power & Energy Systems*, vol. 149, p. 109045, 2023.

[13] L. M. Castro, D. Guillen, and F. Trillaud, "On short-circuit current calculations including superconducting fault current limiters (scfcls)," *IEEE Transactions on Power Delivery*, vol. 33, no. 5, pp. 2513–2523, 2018.

[14] H. Hong, M. Yu *et al.*, "Practical calculation method for the short-circuit current of power grids with high temperature superconducting fault current limiters," *Journal of Electrical Engineering & Technology*, vol. 15, no. 2, pp. 945–953, 2020.

[15] S. Behzadirafi and F. De Leon, "Closed-form determination of the impedance locus plot of fault current limiters: Asymmetrical faults," *IEEE Transactions on Power Delivery*, vol. 35, no. 2, pp. 754–762, 2019.

[16] O. Alsac, B. Stott, and W. Tinney, "Sparsity-oriented compensation methods for modified network solutions," *IEEE Transactions on Power Apparatus and Systems*, no. 5, pp. 1050–1060, 1983.

[17] H. W. Dommel, "Nonlinear and time-varying elements in digital simulation of electromagnetic transients," *IEEE Transactions on Power Apparatus and Systems*, no. 6, pp. 2561–2567, 1971.

[18] A. Haddadi, J. Mahseredjian *et al.*, "Power system test cases for EMT-type simulation studies," CIGRE Working Group C4.503, Tech. Brochure 736, Aug. 2018.

[19] E. Egorova, H. Bahirat *et al.*, "EMTP-ATP modeling of a resistive superconducting fault current limiter," in *International Conference on Power Systems Transients (IPST2013), Vancouver, Canada*, 2013.

[20] W. Romanosky, "Development and testing of a transmission voltage superlimiter™ fault current limiter." [Online]. Available: https://www.osti.gov/biblio/1346952

[21] R. S. Thute, H. J. Bahirat *et al.*, "Line distance protection in the presence of SCFCL," *IET Generation, Transmission & Distribution*, vol. 13, no. 10, pp. 1960–1969, 2019.